

MONTE CARLO MODELING OF ATOMIC OXYGEN ATTACK OF POLYMERS
WITH PROTECTIVE COATINGS ON LDEF

Bruce A. Banks
Kim K. de Groh
Bruce M. Auer
NASA Lewis Research Center
Cleveland, Ohio 44135
Phone: (216) 433-2308 Fax: (216) 433-6106

Linda Gebauer
Jonathan L. Edwards
Cleveland State University
Cleveland, Ohio 44115
Phone: (216) 433-2310 Fax: (216) 433-6106

SUMMARY

Characterization of the behavior of atomic oxygen interaction with materials on the Long Duration Exposure Facility (LDEF) assists in understanding of the mechanisms involved. Thus the reliability of predicting in-space durability of materials based on ground laboratory testing should be improved. A computational model which simulates atomic oxygen interaction with protected polymers has been developed using Monte Carlo techniques. Through the use of an assumed mechanistic behavior of atomic oxygen interaction based on in-space atomic oxygen erosion of unprotected polymers and ground laboratory atomic oxygen interaction with protected polymers, prediction of atomic oxygen interaction with protected polymers on LDEF has been accomplished. However, the results of these predictions are not consistent with the observed LDEF results at defect sites in protected polymers. Improved agreement between observed LDEF results and predicted Monte Carlo modeling can be achieved by modifying of the atomic oxygen interactive assumptions used in the model. LDEF atomic oxygen undercutting results, modeling assumptions, and implications are presented.

INTRODUCTION

Low-Earth-orbital (LEO) atomic oxygen interaction with unprotected and protected polymers has been investigated at low atomic oxygen fluences (approximately 10^{20} atoms/cm²) in space. Results of these in-space tests have provided useful information concerning the erosion yield of unprotected polymers, and the benefits of atomic oxygen protective coatings for low fluence exposures (refs. 1-5). However, no high fluence data exists for protected polymers in LEO other than that generated from a few specimens on LDEF. Although the atomic oxygen protection can be evaluated and erosion yield measurements can be obtained from low

fluence LEO results, this information does not allow confident projection of protected material performance at high fluences, which is needed for long-term LEO missions such as Space Station Freedom (SSF). The inability to project long-term performance of protected polymers based on short-term data is due to the lack of understanding of how scattered atomic oxygen interacts in undercut cavities at defect sites in protective coatings. The data obtained from protected polymers on LDEF provided a unique opportunity to quantify effects of scattered atomic oxygen in undercut cavities at defect sites in protective coatings. Knowledge of the degree of thermal accommodation and erosion yield of thermally accommodated atomic oxygen can potentially be derived by comparing actual LDEF undercut cavity profiles with the Monte Carlo space model and the results of ground-based laboratory testing.

MATERIALS, METHODS, AND PROCEDURE

The procedure used in this investigation consists of an assessment of the validity of mechanistic assumptions used for Monte Carlo modeling of atomic oxygen interaction based on ground laboratory and in-space atomic oxygen exposure of both protected and unprotected polymers.

Ground Laboratory Atomic Oxygen Exposure

Characterization of atomic oxygen interaction with polymers at defect sites in protective coatings has been accomplished using 1300Å-thick SiO_x ($1.9 < X < 2.0$) protective coatings, sputter-deposited on Kapton HN polyimide. Samples were exposed to atomic oxygen in RF plasma ashers (SPI plasma prep II) with air as the working gas. Effects of atomic oxygen undercutting at defect sites in protective coatings were then characterized by scanning electron microscopy before and after removal of the SiO_x thin films over the undercut cavities. Removal of the SiO_x films was accomplished by adhesive tape peelings, which successfully removed the protected SiO_x coating where it was free-standing over undercut defect sites (ref. 6).

In-Space LDEF Atomic Oxygen Exposure

Three types of atomic oxygen protected materials, exposed on the leading edge (row 9) of LDEF, were evaluated by scanning electron microscopy in an effort to obtain atomic oxygen undercutting profiles at defect sites in the protective coatings. Table I describes the protected materials. The aluminized Kapton sample was part of the second layer of a multilayer insulation blanket. The top layer consisted of a sheet of 0.127 mm thick Kapton H, aluminized on the unexposed side only (ref. 7). As a result of atomic oxygen removal of Kapton from the sheet lying above this sample, it was exposed to less than the full leading edge LDEF atomic oxygen fluence. Removal of the aluminum film was accomplished using dilute HC1 to enable scanning electron microscopy examination.

Two carbon fiber epoxy composite samples with protective coatings were analyzed after LDEF exposure on row 9. The protective coating from one carbon fiber epoxy composite sample consisted of $< 1000\text{\AA}$ of Al_2O_3 . The second carbon fiber epoxy composite sample had a protective coating of 400\AA of aluminum on top of 800\AA of chromium.

Monte Carlo Computational Model

A Monte Carlo computational model was developed to predict atomic oxygen undercutting of polymers at the sites of defects in their protective coatings under a variety of environments including LEO and ashers. The model was based on a combination of known and estimated atomic oxygen interaction mechanisms resulting from ground laboratory tests of atomic oxygen undercutting at defect sites in protective coatings and in-space erosion of unprotected polymeric materials (refs. 8-11). The computational model is intended to replicate the effects of atomic oxygen interaction with SiO_x -protected polyimide Kapton at defect sites in the protected Kapton. The Kapton is modeled as an array of square cells for which the behavior of simulated atomic oxygen atoms impinging on each cell is prescribed by a series of assumptions listed below:

1. The model is two-dimensional with atomic oxygen trajectories confined to a plane which simulates the cross-sectional view of a crack or scratch defect in the protective coating.
2. Reaction probability of atomic oxygen with Kapton is proportional to:
 - a. $(\text{energy})^{0.68}$.
 - b. the square root of the cosine of the angle between the surface normal and the arrival direction.
3. Reaction probability at normal incidence is equal to:
 - a. 0.1380 for space (first impact).
 - b. 0.0098 for space (\geq second impact).
 - c. 0.0392 for plasma ashers (first impact).
 - d. 0.0098 for plasma ashers (\geq second impact).
 - e. 0.0490 for plasma ashers and space at Kapton/protective coating interface.
4. Atomic oxygen thermally accommodates upon first impact with surfaces, resulting in reduced reaction probability.
5. Atomic oxygen does not react with protective coatings, nor combines and remains atomic after impacting protective coatings.
6. Unreacted atomic oxygen leaves surfaces in a cosine ejection distribution.
7. Arrival direction of space atomic oxygen is angularly distributed because of the high temperature Maxwellian distribution.
8. Arrival direction of ground laboratory plasma asher atomic oxygen is isotropically distributed.

Several of the above assumptions concerning probability of atomic oxygen reaction after the first impact, energy of the scattered atomic oxygen, and ejection distribution of unreacted atomic oxygen, were optimized to produce good agreement with RF plasma asher results of

atomic oxygen undercutting, without having knowledge of in-space undercutting results. In this paper, atomic oxygen undercutting results from LDEF were used to examine the validity of these assumptions and were used to propose improved assumptions by comparison of predicted LDEF results (based on the previously described assumptions) with the actual LDEF results.

RESULTS AND DISCUSSION

Atomic oxygen undercutting of the LDEF aluminized Kapton multilayer insulation was found to produce undercut cavities which were up to a factor of 2.5-16.6 wider than the width of the aluminized film crack defects (ref. 7). The shape of the undercut cavities shown in figure 1 is rather broad, and would be expected, with isotropic arrival of atomic oxygen, but hardly expected for directed arrival of atomic oxygen. It is probable that the remains of the aluminization of the bottom side of the outermost multilayer insulation blanket contributed to scattering of arriving atomic oxygen which produced arrival trajectories atypical of most unobstructed surfaces on LDEF (ref. 7). As a result, no effort was made to compare the results from this sample with Monte Carlo model undercutting predictions.

Figure 2 is a scanning electron micrograph showing LDEF results of exposure of a T-300 carbon fiber - 934 epoxy composite with a $< 1000\text{\AA}$ -thick Al_2O_3 protective coating. As can be seen by the micrograph, the atomic oxygen protective coating is extremely thin, poorly attached to the substrate, and proliferated with defects, resulting in lack of clear definition of the undercut region for any specific defect site. As a result, no effort was made to compare the results of this sample with Monte Carlo predictions.

Figure 3 is a photograph of the T-300 carbon fiber - 934 epoxy composite sample with an aluminum and chromium protective coating after LDEF exposure. As can be seen in figure 3, the exposed area is a circular region with a slightly darker appearance. In addition, a micrometeoroid or debris impact crater can be seen as a black spot in the upper right section of the photo. The surface texture of the composite sample is highly-quilted as a result of the carbon fiber fabric. This highly irregular surface contributed greatly to the occurrence of defects in the protective coating (ref. 12). Figure 4 is a scanning electron micrograph of a typical defect site prior to and after adhesive tape removal of the aluminum and chromium protective coatings. As can be seen in figure 4, the undercut cavity diameter or width is significantly larger than the respective protective coating defect. Figure 5a and 5b are scanning electron micrographs of a similar defect whose geometry allowed a sufficiently inclined picture to be taken to examine the profile of the crack undercut cavity. Based on similar scanning electron micrographs, a representative undercut cavity profile for crack defects was identified, and is shown in figure 6. Measurement of the area of the undercut cavity shown in figure 6, given the row 9 LDEF atomic oxygen fluence of 8.72×10^{21} atoms/cm², results in an effective erosion yield under the defect site of 2.46×10^{-24} cm³/atom. This erosion yield is approximately twice that of unprotected graphite epoxy based on previous LEO evaluation of carbon fiber epoxy composites (ref. 5). The higher effective erosion yield for atomic oxygen entering defects, compared to atomic oxygen impinging upon unprotected material, is thought to be due to the partial trapping of atomic oxygen within the undercut cavity, which results in multiple opportunities for it to react with the underlying organic material.

Many cracks developed at a 45° angle to the weave pattern. These cracks were more frequently observed in the area exposed to the LEO environment. This implies that some of the cracks may not have been present at the beginning of the in-space exposure, and may therefore have a lower fluence exposure to the underlying composite than others.

A comparison between the observed undercut cavity shown in figure 6, and the Monte Carlo model predicted undercut cavity, required proportioning the undercut-width-to-undercut-cavity-depth ratio so that it would be the same for both the LDEF observed profile and the Monte Carlo predicted profile. This was possible because the Monte Carlo predicted profile was found to vary only in size, but not in shape, once the undercut cavity depth became several times the undercut width. Figure 7 shows an overlay of the observed LDEF undercut profile previously shown in figure 6 and the Monte Carlo model predicted profile based on the previously described Monte Carlo assumptions. As can be seen in figure 7, the width of the Monte Carlo predicted undercut profile is much wider than that experimentally observed. Thus, one must question which assumptions are incorrect in the Monte Carlo model, and how they should be changed to more correctly predict what has been experimentally observed.

Although the Monte Carlo model assumes Kapton as the eroded material, and the actual LDEF material was carbon fiber-epoxy, which has been reported to have a lower erosion yield, the differences in erosion yield are not expected to be sufficient to resolve the differences between observed and predicted results. Reducing the Monte Carlo erosion yield would predominantly only slow down the rate of the development of the undercut cavity and not necessarily the depth-to-width ratio. This is partially based on reference 4, where the reaction probability of carbon is reported to be quite similar to that of Kapton, even though carbon's erosion yield is lower (ref. 4). Perhaps the weakest assumption for the Monte Carlo model is the five times higher reaction probability at the protective coating interface. This assumption was used successfully to predict chamfered undercut cavities for ground laboratory plasma asher results, but it lacks strong mechanistic justification. If one assumes that the Kapton at the interface has the same reaction probability as the bulk, then the chamfer is eliminated, thus producing an undercut cavity closer to the observed space results, but still too wide. The width of the undercut cavity is caused by erosion from scattered atomic oxygen. If one assumes a lower reaction probability for scattered atomic oxygen, then the undercut cavity width predicted by the Monte Carlo model should be smaller. If one assumes that the atomic oxygen thermally accommodates upon impact resulting in 0.04 eV (300 Kelvin) energy atoms, the reaction probability is proportional to the 0.68 power of the oxygen atom energy, and the reaction probability is 0.138 at 4.5 eV (ref. 13), then a reaction probability of 0.006 is predicted for thermally accommodated atomic oxygen. If one assumes that the reaction probability has an Arrhenius relationship, where the activation energy is 0.38 eV as postulated in reference 14, then a reaction probability of 7.7×10^{-6} is predicted for thermally accommodated atomic oxygen. Because a reaction probability of thermally accommodated atomic oxygen of 0.006 was thought to be insufficient to reduce the predicted width of the undercut cavity to match the observed results, atomic oxygen reaction probabilities of 0.0031 and 7.77×10^{-6} were evaluated as shown in figures 8a and 8b. As can be seen by comparison of figures 8a and 8b, the reaction probability of 0.0031 for atomic oxygen reacting with the composite after the first impact produces an undercut cavity profile much closer to that which is experimentally observed than the much lower reaction probability shown in figure 8b. Thus, based on figure 8, one can

conclude that the reaction probability of thermally accommodated atomic oxygen should be less than or equal to 0.003.

There may be other Monte Carlo assumptions which produce undercut profiles which approximate the observed LDEF results such as the degree to which energetic atomic oxygen arriving at 4.5 eV thermally accommodates upon its first impact. If one assumes that only a portion of the atomic oxygen thermally accommodates upon first impact, then higher reaction probabilities of more energetic scattered atomic oxygen will result, thus widening the undercut cavity in comparison to figure 8b. Figure 9 compares the observed LDEF undercut cavity profile and the Monte Carlo predicted profile for atomic oxygen, which is assumed to have only a 50% probability of accommodation upon each impact and the same low reaction probability as figure 8b for thermally accommodated atomic oxygen. The fraction of atoms which did not accommodate, and also did not react, were assumed to specularly scatter, retaining their initial energy. The fraction of atoms which did accommodate were assumed to scatter in a cosine distribution with thermally accommodated energies. As can be seen in figure 9, energetic scattering of atomic oxygen significantly widens the undercut cavity profile, even if the thermally accommodated reaction probability is negligible. Thus, it is quite possible that partial accommodation of atomic oxygen could occur upon first impact, provided that the fully accommodated atomic oxygen has a very low reaction probability.

CONCLUSION

A comparison was made between a Monte Carlo predicted undercut cavity profile for cracks in protected carbon fiber epoxy composite materials with experimentally observed results from an LDEF row 9 exposure to an atomic oxygen fluence of 8.72×10^{21} atoms/cm². These results indicate that the atomic oxygen erosion yield under defect sites in protective coatings on carbon fiber epoxy composites is 2.5×10^{-24} cm³/atom, which is approximately twice that which is observed for unprotected carbon fiber epoxy composites. Monte Carlo modeling assumptions which result in predictions that replicate ground laboratory plasma asher results do not accurately predict LDEF results. Based on the LDEF results, several mechanistic assumptions used in the Monte Carlo modeling should be altered to produce in-space predictions which more accurately reflect experimentally observed results. The reaction probability of atomic oxygen with polymeric material at the interface between the protective coating and the polymer appears to be the same as for the bulk materials. The atomic oxygen reaction probability for thermally accommodated atomic oxygen is probably not greater than 0.003. The atomic oxygen may not fully accommodate upon first impact with organic materials, thus scattering with sufficient energy to significantly contribute to undercutting.

ACKNOWLEDGEMENTS

The authors gratefully acknowledge the assistance of Phillip Young and Wayne Slemp of the NASA Langley Research Center for kindly providing the samples of LDEF materials used for this paper.

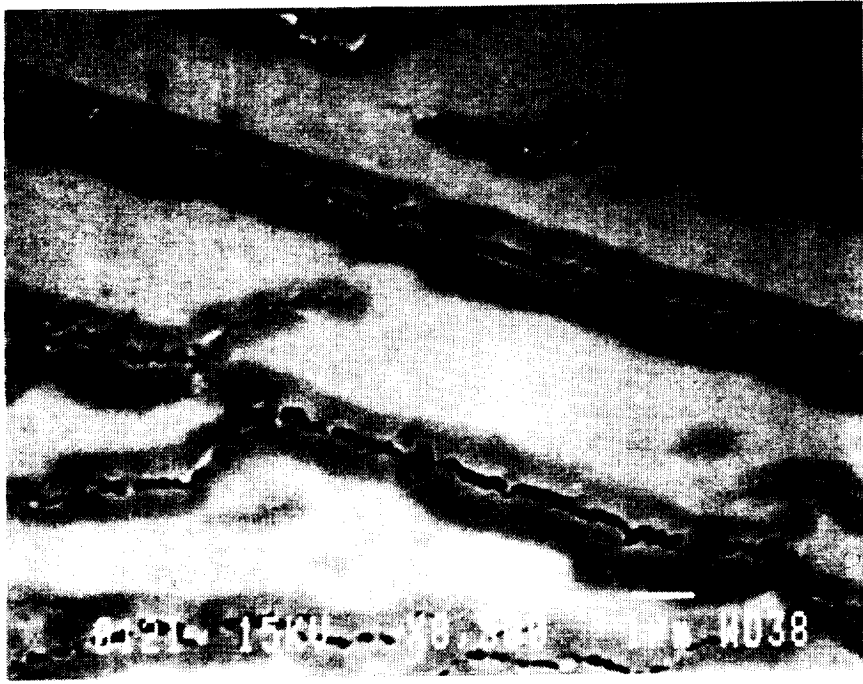
REFERENCES

1. L.J. Leger, "Oxygen Atom Reaction with Shuttle Materials at Orbital Altitudes," NASA TM-58246, 1982.
2. J.T. Visentine, L.J. Leger, J.F. Kuminecz, and I.K. Spiker, "STS-8 Atomic Oxygen Effects Experiment," AIAA Paper 85-0415, AIAA 23rd Aerospace Sciences Meeting, Reno, Nevada, January 14-17, 1985.
3. B.A. Banks, M.J. Mirtich, S.K. Rutledge, D.M. Swec, and H.K. Nahra, "Ion Beam Sputter-Deposited Thin Film Coatings for the Protection of Spacecraft Polymers in Low Earth Orbit," NASA TM-87051, paper presented at the 23rd Aerospace Sciences Meeting, Reno, Nevada, January 14-17, 1985.
4. D.E. Brinza, "Proceedings of the NASA Workshop on Atomic Oxygen Effects," JPL Publication 87-14 (June 1, 1987), Pasadena, California, November 10-11, 1986.
5. B.A. Banks and S.K. Rutledge, "Low Earth Orbital Atomic Oxygen Simulation for Materials Durability Evaluation," proceedings of the 4th European Symposium on Spacecraft Materials in a Space Environment, CERT, Toulouse, France, September 6-9, 1988.
6. B.A. Banks, S.K. Rutledge, L. Gebauer, and C. LaMoreaux, "SiO_x Coatings for Atomic Oxygen Protection of Polyimide Kapton in Low Earth Orbit," AIAA Paper 92-2151 proceedings of the Coatings Technology for Aerospace Systems Materials Specialists Conference, Dallas, Texas, April 16-17, 1992.
7. K.K. de Groh and B.A. Banks, "Atomic Oxygen Undercutting of LDEF Aluminized-Kapton Multilayer Insulation," proceedings of the First LDEF Post-Retrieval Symposium, NASA CP-3134, Kissimmee, Florida, June 2-8, 1991.
8. B.A. Banks, S.K. Rutledge, B.M. Auer, and F. DiFilippo, "Atomic Oxygen Undercutting of Defects on SiO₂ Protected Polyimide Solar Array Blankets," Published in Materials Degradation in Low Earth Orbit (LEO), edited by V. Srinivasan and B.A. Banks (The Minerals, Metals, and Materials Society), pp. 15-33, 1990.
9. B.A. Banks, B.M. Auer, S.K. Rutledge, and C. Hill, "Atomic Oxygen Interaction with Solar Array Blankets at Protective Coating Defect Sites," paper presented at the 4th Annual Workshop on Space Operations, Automation, and Robotics (SOAR '90), Albuquerque, New Mexico, June 26-29, 1990.
10. B.A. Banks, S.K. Rutledge, K.K. de Groh, B.M. Auer, M.J. Mirtich, L. Gebauer, C. Hill, and R. Lebed, "LDEF Spacecraft, Ground Laboratory, and Computational Modeling Implications on Space Station Freedom's Solar Array Materials and Surfaces Durability," proceedings of the IEEE Photovoltaic Specialists Conference, Las Vegas, Nevada, October 7-11, 1991.

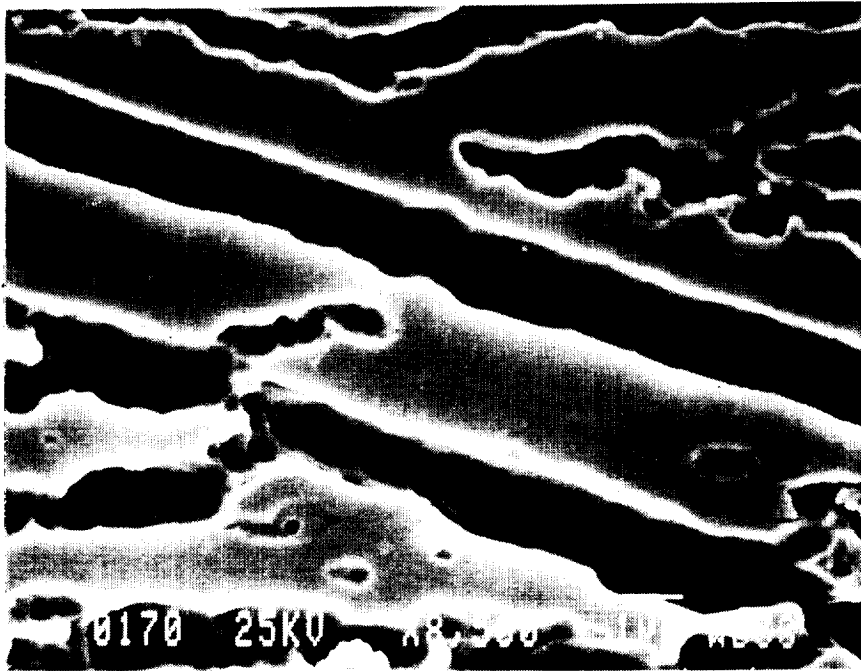
11. B.A. Banks, B.M. Auer, S.K. Rutledge, L. Gebauer, and E.A. Sechkar, "Monte Carlo Modeling of Atomic Oxygen Interaction with Protected Polymers for Projection of Materials Durability in Low Earth Orbit," proceedings of the MRS Spring Meeting '92, San Francisco, California, April 27-May 1, 1992.
12. K.K. de Groh, T. Dever, and W. Quinn, "The Effect of Leveling Coatings on the Atomic Oxygen Durability of Solar Concentrator Surfaces," proceedings of the 8th International Conference on Thin Films (ICTF-8) and the 17th International Conference on Metallurgical Coatings (ICMC-17), San Diego, California, April 2-6, 1990.
13. D.C. Ferguson, "The Energy Dependence of Surface Morphology of Kapton Degradation Under Atomic Oxygen Bombardment," paper presented at the 13th Space Simulation Conference, Orlando, Florida, October 8-11, 1984.
14. S. Koontz, K. Albyn, and L.J. Leger, "Atomic Oxygen Testing with Thermal Atom Systems: A Critical Evaluation," Journal of Spacecraft and Rockets, Vol. 28, No. 3, May-June, 1991.

Table I. LDEF Samples Evaluated Having Atomic Oxygen Protective Coating

SUBSTRATE	ATOMIC OXYGEN PROTECTIVE COATING
0.0076 mm thick Kapton H	1000Å thick aluminum on both surfaces
0.41 mm thick T300 carbon fiber - 934 epoxy composite	< 1000Å thick Al ₂ O ₃
0.64 mm thick T300 carbon fiber - 934 epoxy composite	400Å thick aluminum over 800Å of chromium



1a. With aluminum.



1b. Aluminum chemically removed.

Figure 1. Atomic oxygen undercutting of LDEF aluminized Kapton multilayer insulation at cracks in the aluminum film.

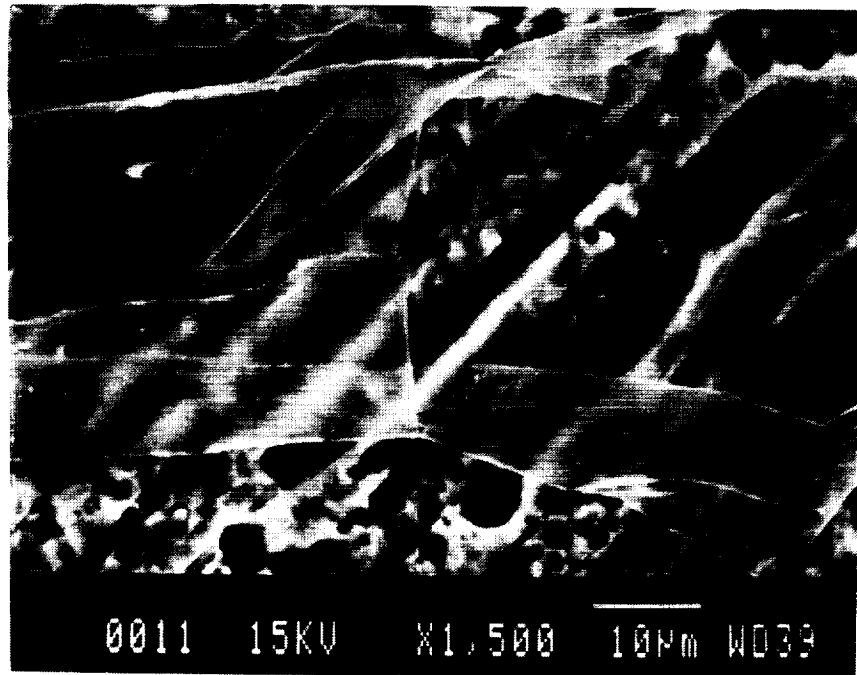


Figure 2. Scanning electron micrograph of $< 1000\text{\AA}$ -thick SiO_x T-300 carbon fiber - 934 epoxy composite after LDEF exposure to an atomic oxygen fluence of 8.72×10^{21} atoms/cm².

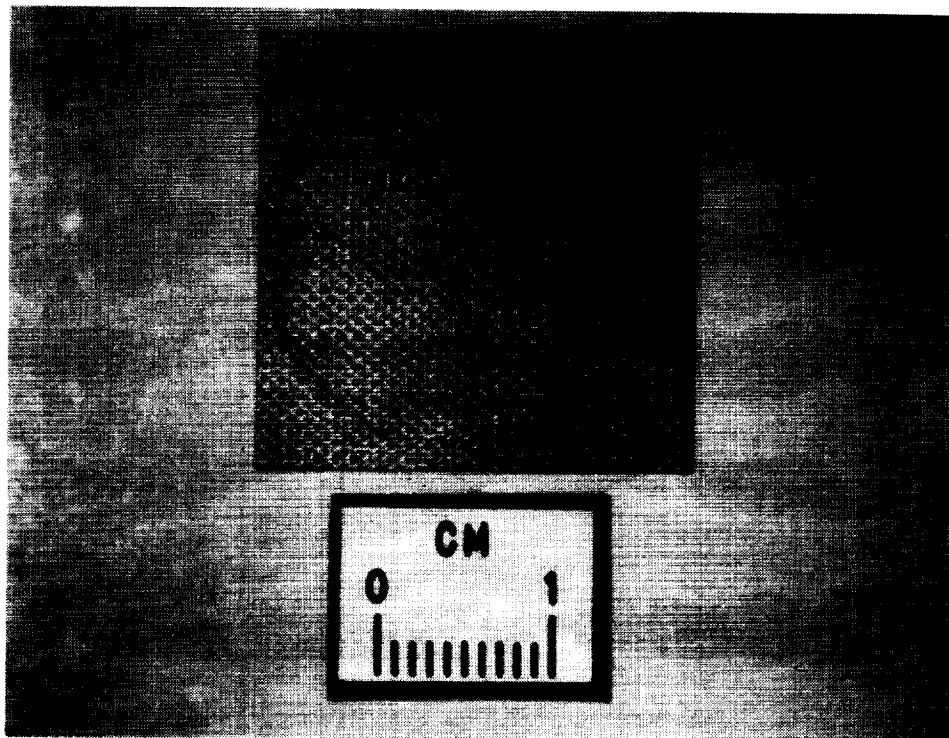
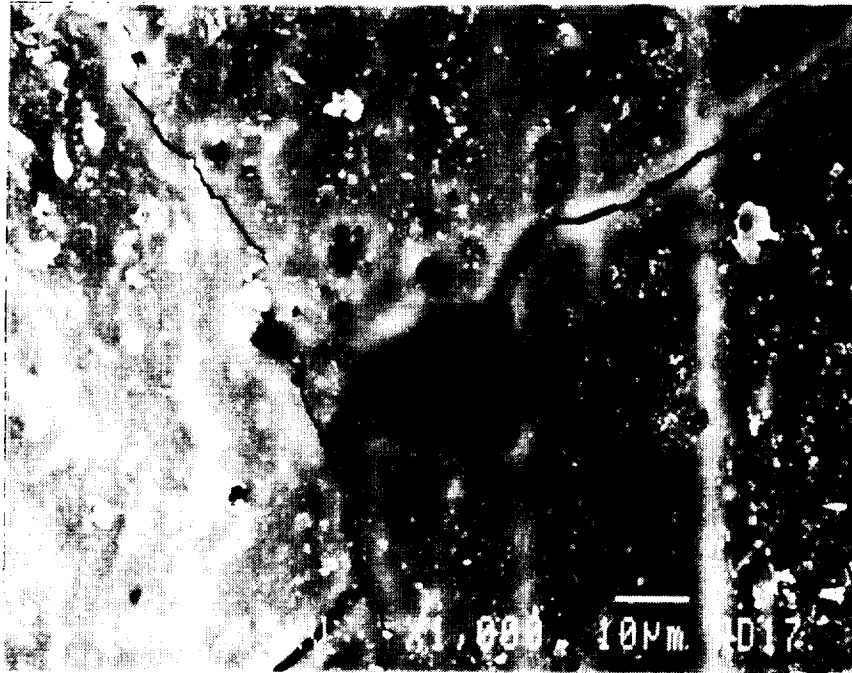
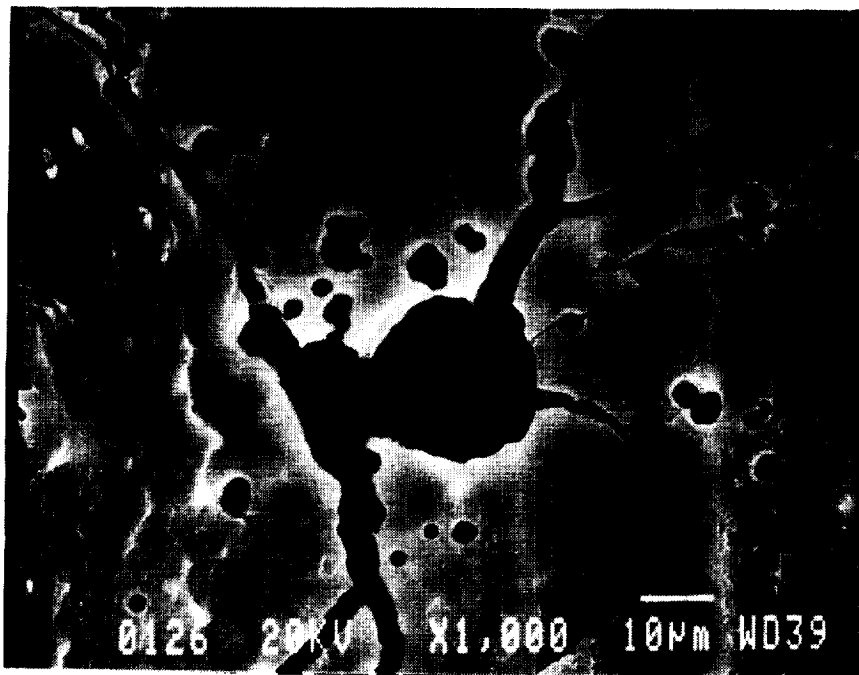


Figure 3. Photograph of 400\AA Al/ 800\AA Cr coated T-300 carbon fiber - 934 epoxy composite after LDEF exposure to an atomic oxygen fluence of 8.72×10^{21} atoms/cm².



4a. Prior to removal of aluminum/chromium protective coating.

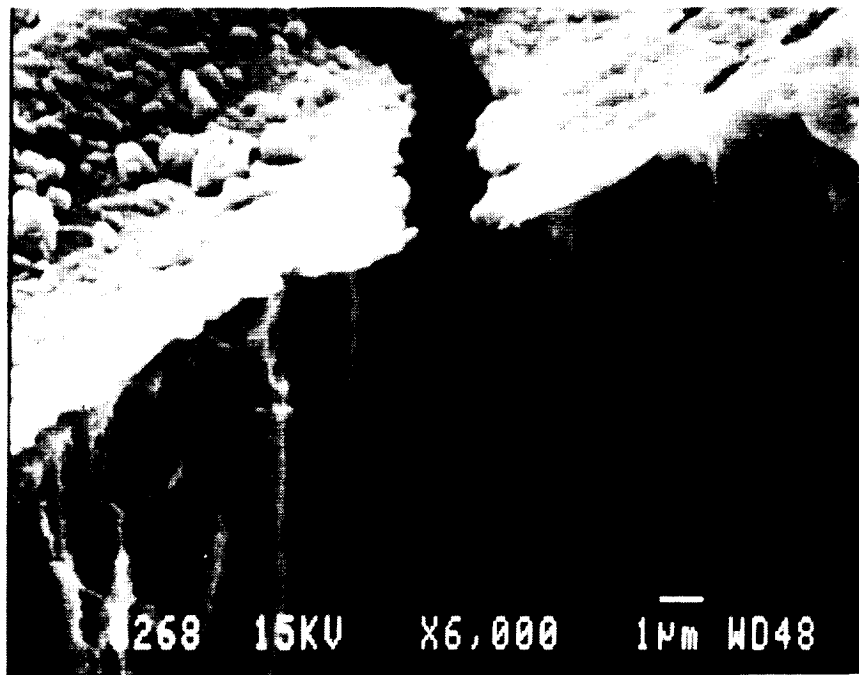


4b. After removal of aluminum/chromium protective coating.

Figure 4. Scanning electron micrograph of aluminum/chromium coated T-300 carbon fiber - 934 epoxy composite after LDEF exposure.



5a. Low magnification



5b. High magnification

Figure 5. Scanning electron micrograph of aluminum/chromium coated T-300 carbon fiber - 934 epoxy composite after LDEF exposure showing crack undercut cavity profile.

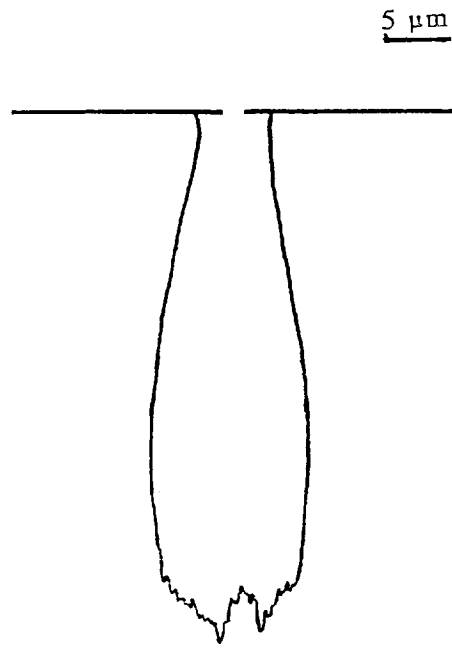


Figure 6. Crack defect undercut cavity profile based on scanning electron micrographs similar to figure 5.

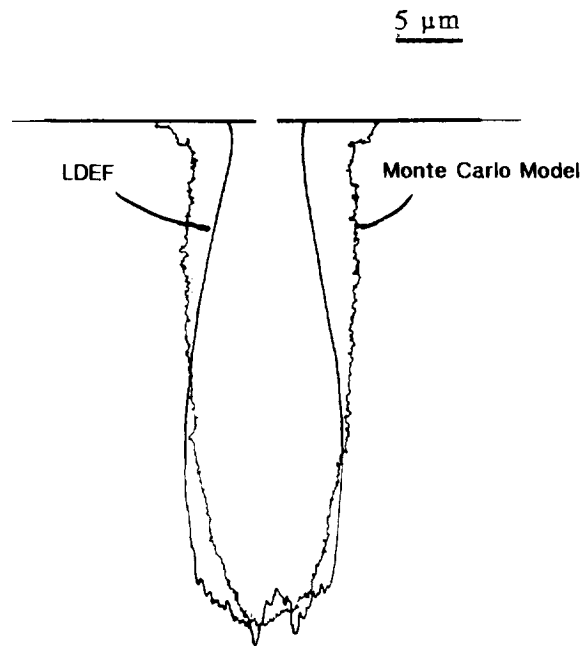
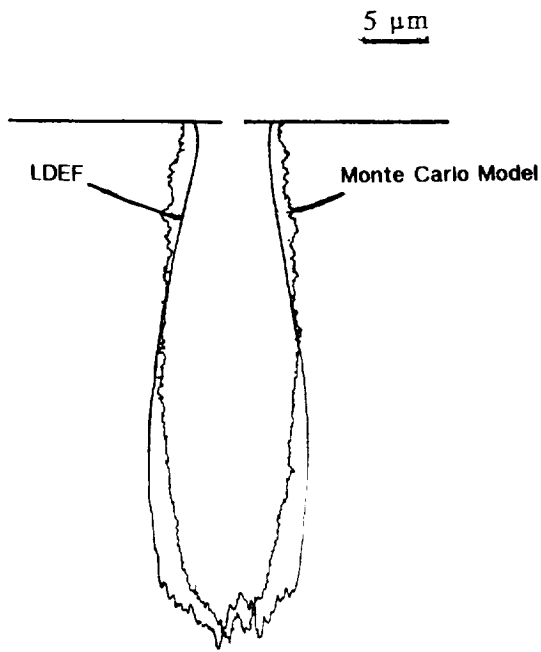
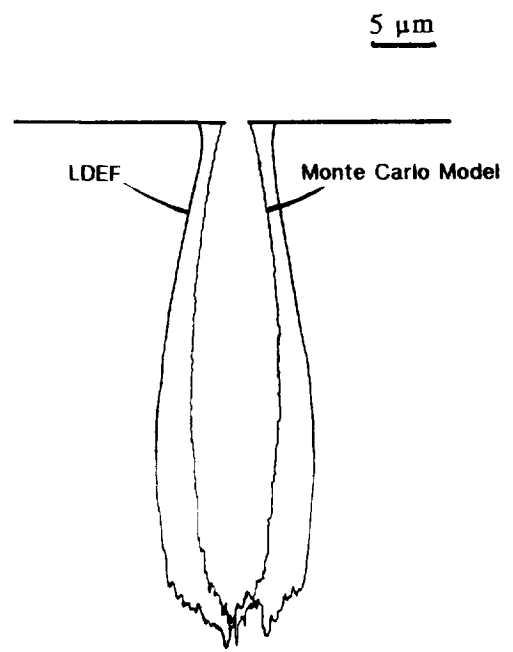


Figure 7. Comparison of LDEF undercut cavity profile and Monte Carlo predicted profile based on atomic oxygen: 100% accommodation, reaction probability of 0.0098 for greater than or equal to second impact, and reaction probability of 0.0490 at the protective coating interface.



8a. Reaction probability of 0.0031 for \geq second impact.



8b. Reaction probability of 7.77×10^{-6} for \geq second impact.

Figure 8. Comparison of LDEF undercut cavity profiles and Monte Carlo predicted profiles based on atomic oxygen: 100% accommodation and reaction probability at the protective coating interface equal to the bulk.

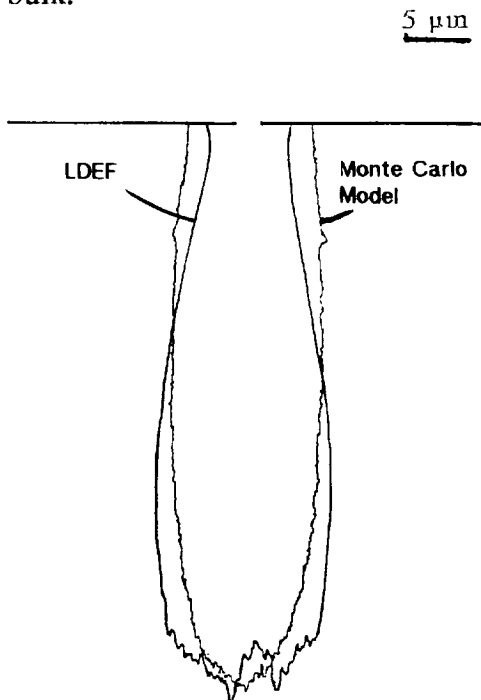


Figure 9. Comparison of LDEF undercut cavity profile and Monte Carlo predicted profile based on atomic oxygen: 50% accommodation, reaction probability of 7.77×10^{-6} for \geq second impact, and reaction probability at the protective coating interface equal to the bulk.